Bioelectrochemistry 141 (2021) 107847

Contents lists available at ScienceDirect

Bioelectrochemistry

journal homepage: www.elsevier.com/locate/bioelechem

Contactless delivery of plasmid encoding EGFP *in vivo* by high-intensity pulsed electromagnetic field

Matej Kranjc [a,#], Simona Kranjc Brezar [b,c,#], Gregor Serša [b,d], Damijan Miklavčič [a,*]

[a] University of Ljubljana, Faculty of Electrical Engineering, Trzaska 25, SI-1000 Ljubljana, Slovenia
[b] Institute of Oncology Ljubljana, Department of Experimental Oncology, Zaloska 2, SI-1000 Ljubljana, Slovenia
[c] University of Ljubljana, Faculty of Medicine, Vrazov trg 2, SI-1000 Ljubljana, Slovenia
[d] University of Ljubljana, Faculty of Health Sciences, Zdravstvena pot 5, SI – 1000 Ljubljana, Slovenia

ARTICLE INFO

Article history:
Received 31 December 2020
Received in revised form 14 May 2021
Accepted 18 May 2021
Available online 24 May 2021

Keywords:
Magnetic fields
Electric fields
Membrane permeabilization
Electroporation
Enhanced green fluorescent protein
Mouse melanoma model

ABSTRACT

High-Intensity Pulsed Electromagnetic Fields (HI-PEMF) treatment is an emerging noninvasive and contactless alternative to conventional electroporation, since the electric field inside the tissue is induced remotely by external pulsed magnetic field. Recently, HI-PEMF was applied for delivering siRNA molecules to silence enhanced green fluorescent protein (EGFP) in tumors *in vivo*. Still, delivered siRNA molecules were 21 base pairs long, which is 200-times smaller compared to nucleic acids such as plasmid DNA (pDNA) that are delivered in gene therapies to various targets to generate therapeutic effect. In our study, we demonstrate the use HI-PEMF treatment as a feasible noninvasive approach to achieve *in vivo* transfection by enabling the transport of larger molecules such as pDNA encoding EGFP into muscle and skin. We obtained a long-term expression of EGFP in the muscle and skin after HI-PEMF, in some mice even up to 230 days and up to 190 days, respectively. Histological analysis showed significantly less infiltration of inflammatory mononuclear cells in muscle tissue after the delivery of pEGFP using HI-PEMF compared to conventional gene electrotransfer. Furthermore, the antitumor effectiveness using HI-PEMF for electrotransfer of therapeutic plasmid, i.e., silencing MCAM was demonstrated. In conclusion, feasibility of HI-PEMF was demonstrated for transfection of different tissues (muscle, skin, tumor) and could have great potential in gene therapy and in DNA vaccination.

1. Introduction

Several medical applications for both diagnosis and therapy rely on the application of pulsed electromagnetic fields [1]. Most of the studies employing pulsed electromagnetic fields are focused on low-intensity magnetic fields, such as FDA approved healing non-union or delayed bone fractures [2,3]. Transcranial magnetic stimulation (TMS) is the exception as it utilizes time-varying high-intensity pulsed electromagnetic fields (HI-PEMF) to deliver highly localized brain stimulations by inducing an electric field in the human cortex [4,5]. This non-invasive and painless technique provides researchers and clinicians with a unique tool capable of stimulating both central and peripheral nervous systems [6,7]. In recent years, several studies demonstrated that HI-PEMF primarily used for TMS can also be applied for non-invasive permeabilization of the cell membrane [8-10]. One of the first studies on the possible effect of electromagnetic pulses on cell membrane permeability showed that time-varying magnetic field exposure of 2.2 T peak strength increases transmembrane molecular transport [11]. Pulsed electromagnetic fields were successfully applied in studies *in vitro* for reversible permeabilization of biological cells [8,12] and in studies *in vivo*, where the feasibility and antitumor effectiveness of magnetic pulses as a drug delivery system for cisplatin to murine melanoma subcutaneous tumors was evaluated [10]. Results showed that even a magnetic field below 1 T was sufficient to achieve membrane permeabilization of tumor cells and that the antitumor effect in treatment with pulsed electromagnetic field was related to increased drug uptake into tumor cells as demonstrated by the increased amount of platinum bound to the DNA. Mechanisms and pathways of increased molecular transmembrane transport induced by the HI-PEMF are however not known. The observed effect is similar to increased membrane permeabilization triggered by conventional electroporation, a process in which cells are exposed to high-intensity electric field pulses (hundreds of V/cm) for a short duration (μs-ms) [13]. But in all of the above-mentioned studies on HI-PEMF, the induced electric field value

* Corresponding author.
E-mail address: damijan.miklavcic@fe.uni-lj.si (D. Miklavčič).
# Matej Kranjc and Simona Kranjc Brezar both are contributed equally to this paper.

https://doi.org/10.1016/j.bioelechem.2021.107847
1567-5394/

was at best 2.12 V/cm for *in vitro* studies [12] and 0.24 V/cm for *in vivo* studies [9], which is at least two orders of magnitude lower from what is usually reported as the electric field threshold leading to membrane electroporation.

Recently, HI-PEMF was applied for delivering siRNA molecules to silence enhanced green fluorescent protein (EGFP) in B16F10-EGFP tumors *in vivo* [9]. Since siRNA delivery is a promising gene therapy approach for inactivating oncogenes and tumor suppressor genes involved in cancer disease [14], the results obtained in the *in vivo* mouse model demonstrate the potential use of HI-PEMF for cancer therapy. Still, delivered siRNA molecules were 21 base pairs long, which is 200-times smaller compared to nucleic acids such as plasmid DNA that are delivered in gene therapies to various targets to generate therapeutic effect [15,16]. The simplest way of delivery is a direct injection of naked plasmid DNA into targeted tissue [17]. However, since the expression level after injection of naked plasmid DNA is generally limited, various physical approaches have been introduced to improve efficiency, such as electroporation, balistics, ultrasound, hydrodynamics and others [18,19]. Among them, electroporation (also referred to as electrotransfer) provides the most substantial change in the efficiency of plasmid-gene transfer [20]. Electroporation *in vivo* increases the transfection 100–10.000x in terms of gene expression [21,22], >100x in terms of serum protein levels [22,23], and 10-100x in terms of the number of transfected muscle fibers [21,24] compared to DNA injection alone. Furthermore, it strongly reduces intersubject variability [21,22] and was shown to be a powerful adjuvant in DNA vaccination [25]. Still, one of the drawbacks of electrotransfer that limits the efficiency of transfection is the tissue damage associated with the procedure, especially if electric pulse parameters are not appropriately chosen [26,27]. Another is the presence of electrochemical reactions in the electrode–electro lyte/tissue interface and alteration of the pH, potentially causing denaturation of the plasmid DNA [28-30]. The HI-PEMF approach of plasmid DNA delivery could have an advantage over conventional electroporation since HI-PEMF is non-invasive, contactless, and painless. Therefore, we explored HI-PEMF contactless delivery technique for electrotransfer of bigger molecules, i.e., plasmid DNA, by evaluating the transfection efficiency of plasmid DNA encoding EGFP (pEGFP-N1) in mouse muscle, skin, and tumor *in vivo*. In addition, a plasmid DNA encoding shRNA against melanoma cell adhesion molecule (MCAM), as a therapeutic approach in gene electrotransfer (GET) mediated by HI-PEMF, in the melanoma B16F10 tumor model was used to compare its antitumor effectiveness to conventional GET using contact electrodes.

2. Material and methods

2.1. Experimental design

Mice were randomly divided into 4 experimental groups: a group subject to single intramuscular or intradermal injection of endotoxin-free water combined with HI-PEMF treatment (HI-PEMF), a group subject to single intramuscular or intradermal injection of pEGFP-N1 (EGFP), a group subject to single intramuscular or intradermal injection of pEGFP-N1 combined with either HI-PEMF treatment (HI-PEMF + EGFP) or conventional electroporation (EP/GET + EGFP). Changes in the EGFP expression in muscles (left and right hind leg) and skin (left and right flank) of 72 mice were evaluated through the skin utilizing non-invasive stereomicroscopy fluorescence imaging at different time points Specifically, 24 animals were used for long term expression of EGFP and histology (up to 230 days after the treatment) and for the other short term expression and histology 24 animals per each time point (2 days and 5 days). At these time points after the treatment, animals were humanely sacrificed, the muscle tissues were carefully removed and imaged for precise evaluation of transfection.

Antitumor response to pMCAM was evaluated on 62 mice that were randomly divided into 9 experimental groups: an untreated control group (Control, n = 6), tumors exposed to conventional electric pulses (EP group, n = 6) or to application of high intensity of pulsed electromagnetic fields (HI-PEMF group, n = 6) alone, tumors treated with intratumorally injection of plasmid DNA encoding shRNA against MCAM (pMCAM group, n = 6) or intratumorally injection of control plasmid (pControl group, n = 6), tumors exposed to treatment with conventional electroporation and intratumoral injection of pMCAM (GET pMCAM group, n = 8) or intratumoral injection of pControl (GET pControl, n = 8) and tumors exposed to treatment with HI-PEMF and intratumoral injection of pMCAM (HI-PEMF pMCAM group, n = 8) or intratumoral injection of pControl (HI-PEMF pControl, n = 8). Each therapy was performed three times (on day 0, 2 and 4).

2.2. Plasmid DNA (pEGFP-N1, pMCAM, pControl)

In the experiments for optimization of transfection protocol by HI-PEMF in different tissues (tumor, muscle or skin) a plasmid DNA encoding EGFP (Clontech Laboratories, Inc., Mountain View, CA, USA) was used. Further, to evaluate the HI-PEMF as a potential delivery method of a therapeutic gene into the tumors two plasmids with constitutive CMV promoter were used, therapeutic plasmid DNA encoding shRNA against MCAM (pMCAM; pENTR/U6 CD146) [31] and control plasmid DNA, encoding shRNA with no homology to any gene in the mouse genome as a negative control (pControl; pENTR/U6 pControl) [32]. Plasmids were isolated using a Qiagen® Endo-Free Plasmid Mega Kit (Qiagen, Hilden, Germany) and dissolved in sterile endotoxin-free water to a final concentration of 2 μg/μl or 4 μg/μl.

2.3. Mice, tumor models

Female C57Bl/6 and SKH1-Elite mice (Envigo RMS S.r.l., San Pietro al Natisone, Italy) were maintained in quarantine for 2–3 weeks. The mice were kept at constant room temperature with a 12 h light cycle. In the experiments, 8- to 9-week-old mice weighing 20–22 g were used. All animal experimental manipulations were conducted according to the principles and following procedures outlined in the guidelines for animal experiments of the EU directives (2010/63/EU and 86/609/EEC) and with permission from The Administration of the Republic of Slovenia for Food Safety, Veterinary and Plant Protection (The Republic of Slovenia, The Ministry of Agriculture, Forestry and Food) (permission No: U34401–1/2015/43).

The *tibialis cranialis* muscle and skin area (diameter 1 cm) on the flank of SKH1-Elite mice were used in the experiments with pEGFP-N1. In addition, B16F10 melanoma tumors were implanted subcutaneously into the C57Bl/6 mice in the right flank of the mice by inoculation of a suspension 1×10^6 B16F10 melanoma cells prepared in 100 μl of PBS for experiments silencing MCAM with HI-PEMF and conventional gene electrotransfer (GET). The optimization procedures were performed in BALB/c and C57Bl/6 female mice, which are described in Supplemetary data.

2.4. In vivo delivery of plasmid DNA (pEGFP-N1 or pMCAM, pControl)

The skin area over the *tibialis cranialis* muscle on the left and right hind leg, over the tumor and the skin on the flank of mice were depilated (Reckitt Benckiser Health Care Ltd). After the animals were anesthetized, 15 μl (30 μg) of pEGFP-N1 was injected intramuscularly through the skin (medial anterior position) or intradermally in the skin. In the combined treatment schedule,

the muscle or skin was exposed to the treatment with either HI-PEMF or conventional electroporation 10 s after the injection. In the case of tumors as target tissue, 25 μl (50 μg) plasmid DNA (pMCAM, pControl) was slowly injected intratumorally followed by HI-PEMF or conventional electroporation applied after 10 min.

2.5. Gene transfer using High-Intensity pulsed electromagnetic field

HI-PEMF was delivered by a custom-made magnetic field pulse generator connected to an applicator consisting of a round coil with 68 turns. The generator supplied the applicator with bipolar electric pulses that generated a time-varying HI-PEMF in the vicinity of the coil (Fig. 1). The applicator was positioned over the treated tissue so that the treated tissue was located at the periphery of the coil just below the middle of the windings where the induced electric field is the highest. To improve induced electric field in the tissue, we added conductive gel (G006 ECO, FIAB, Vicchio, Italy) between the applicator and tissue in order to decrease opposing electric field established in the tissue due to charge accumulation on air-tissue boundary [33]. The pulse sequences of electric current delivered to the applicator consisted of 400 bipolar pulses at the repetition frequency of 33 Hz (the application of HI-PEMF lasted a total of 12 s). The optimization procedures of HI-PEMF are described in Supplementary material.

2.6. Gene electrotransfer

For gene electrotransfer, different electric pulse parameters and electrodes were applied. The electric pulse parameters for muscle gene electrotransfer were chosen based on the study of Tevz *et al*, where efficient and long-term gene expression in muscle was demonstrated [27]. Briefly, the muscle was placed between plate electrodes 4 mm apart immediately after the plasmid DNA intramuscular injection and exposed to square wave electric pulses: one high voltage (HV, 600 V/cm, 100 μs long) followed by four low voltage (LV, 80 V/cm, 100 ms long) at a frequency of 1 Hz [27]. In the skin, GET was performed immediately after the intradermal injection of plasmid DNA using 24 electric pulses (570 V, 100 μs long) at 5 kHz, that are known to provide gene expression in the superficial skin layers and induced a local response [34]. The electric pulses were delivered through a noninvasive multi-electrode array consisting of 7 spring-loaded pins arranged in a hexagonal mesh and spaced 3.5 mm apart from each other. For conventional GET in the muscle and skin, a CLINIPORATOR^{TM} electric pulse generator (IGEA s.r.l., Carpi, Italy) was used. In tumors, GET was performed 10 min after intratumoral injection of plasmid DNA. Tumors were placed between plate electrodes 6 mm apart and exposed to eight square-wave electric pulses (600 V/cm, 5 ms, 1 Hz; β Tech, Leroy, France). The electric pulse parameters were chosen based on the studies Kranjc Brezar *et al* [35], where the expression of the transgene at protein and mRNA level, as well as the antitumor effectiveness of the transgene were determined. Good contact between the electrodes and the skin over the muscle, over the tumor or the skin on the back of the animal, was ensured by the use of conductive gel (G006 ECO, FIAB, Vicchio, Italy).

2.7. Assessment of the EGFP expression

EGFP expression in muscles and skin was evaluated utilizing non-invasive stereomicroscope fluorescence imaging using Carl Zeiss SteREO Lumar V12 fluorescence stereomicroscope equipped with a NeoLumar S 0.8× objective and an AxioCam MRc5 digital camera (all from Carl Zeiss, Jena, Germany). This equipment allowed the observation of the EGFP expression in the same animal for several days. The animals were anesthetized with isoflurane inhalation anesthesia and placed on a custom-designed holder. Aiming to achieve the best conditions for *in vivo* imaging in the treated tissue, the targeted area was shaved and depilated. The exposure time was set at 2 s with no binning. The EGFP fluorescence from the treated tissue was quantitatively evaluated at the measured time points. From the bright-field images acquired at 12.5× magnification, the target tissue was located and manually gated to determine the region of interest. For the images taken with the GFP filter, a suitable threshold was applied, and the fluorescence intensity in the whole area of the target tissue, i.e., the region of interest determined from bright-field images, was determined with image analysis software ImageJ/Fiji (National Institutes of Health, Bethesda, MD, USA) [36]. Besides, the expression of EGFP in the upper layer of skin was determined by noninvasive imaging confocal laser scanning microscope equipped with a water immersion objective W Plan-Apochromat 20 × 1.0 DIC and GaAsP wavelength detector 485–700 nm (Examiner. Z1, Zeiss LSM 800, Zeiss, Germany) and an AxioCam 506 color digital camera 2, 7 and 14 days after the transfection using HI-PEMF. A laser was used for excitation at 488 nm (green signal) and a signal was acquired for each slice/time-point. First, the z-stack was acquired with a spacing of 1 μm between slices to obtain a 3D image of the skin in the treated area, starting at the the top and finished in total 152 μm of skin thickness.

2.8. Histological assessment of transfected tissue

To evaluate tissue damage in muscle tissue caused by the treatment, muscles were removed at different time intervals after the procedure to assess early tissue damage (2 days), as well as late tissue damage (6 months). The harvested muscles were cross sectioned in the middle (horizontal direction) and fixed in Zn-fixativ for 24 h, afterward placed in 70% of ethanol for 24 h and embedded in paraffin blocks that were cut into tissue sections of 10 μm. Ten consecutive sections per muscle were cut. Tissue sections were differentially stained with hematoxylin-eosin dye. The extent of histological change was determined as a fraction of the area with inflammatory mononuclear cell infiltration concerning the whole muscle area. Besides, muscles were inspected for the presence of necrosis. Images of muscle sections (5 fields of view/section) were captured by a digital color camera (Olympus, Hamburg, Germany) and analyzed with CellSens Dimension software. The field of view did not include the site of injection, but it is at the site of treatment and expression.

2.9. Assessment of antitumor response to pMCAM

Three orthogonal diameters (a, b, c) of tumors were measured by Vernier caliper every second day and the tumor volume was calculated according to the formula $V = a \times b \times c \times \pi/6$. From the tumor volumes, arithmetic means and standard error of the mean for each group were calculated. The antitumor effect was assessed by tumor doubling time (DT), determined as the time in which the tumor doubled the volume from the initial day of the experiment. In addition, the tumor growth delay (GD) was calculated as the difference in tumor DT of the therapeutic and control group. The growth of tumors was followed until the tumor volume reached 400 mm^3 (data used growth curves). The animals were assigned as cured if they were tumor-free until 100 days after the treatment. Thereafter, cured animals were challenged with a secondary subcutaneous injection of the B16F10 melanoma cells as described above in the left flank. The outgrowth of tumors was followed till 100 days after the injection of tumor cells and the animals were considered as resistant to secondary challenge if no tumor growth at day 100 was observed. Animal weight loss was monitored as a sign of systemic toxicity of the treatments.

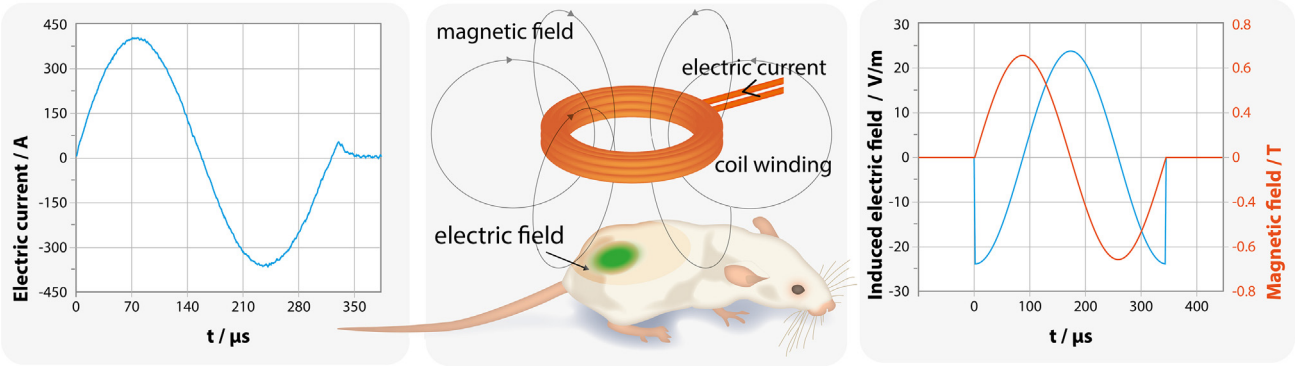

Fig. 1. Time-varying current (left figure) through the coil (central figure) induces a time-varying magnetic field (orange line, right figure) which in turn induces an electric field in the tissue (blue line, right figure). This electric field then presumably causes membrane permeabilization. No electrodes and contact are thus needed. Values of induced electric and magnetic field correspond to the application of HI-PEMF on location L_b in the muscle (see Figure S1 in Supplementary).

2.10. Statistical analysis

All data were tested for a normal distribution with the Shapiro–Wilk test (α = 0.05). A one-way analysis of variance (ANOVA) followed by a Holm-Sidak test or unpaired, nonparametric Mann-Whitney test was used to evaluate the differences between the experimental groups. A P-value of <0.05 was considered significant. SigmaPlot software (Systat Software, Chicago, IL, USA) was used for statistical analysis and graphical presentation.

3. Results

3.1. Assessment of the EGFP expression in tibialis cranialis muscle and skin

To test whether HI-PEMF enables gene transfer to *tibialis cranialis* muscle and skin, the HI-PEMF was performed immediately (10 s) after intramuscular or intradermal injection of plasmid pEGFP-N1 in SKH1 hairless mice. The HI-PEMF treatment was compared to conventional electroporation using high voltage square wave electric pulses delivered via plate electrodes to muscle or via a multi-electrode array to the skin. The transfection efficiency was noninvasively assessed by fluorescence stereomicroscope imaging at different time points. One third of the animals were humanely sacrificed 5 days after the treatment for a precise evaluation of transfection. Altogether, the expression of EGFP after HI-PEMF application was observed in both *tibialis cranialis* muscle (Fig. 2) and skin (Figs. 3 and 4). As expected, no expression of EGFP was observed in any of the control groups: plasmid DNA (EGFP) injection only or application of HI-PEMF only. The fluorescent intensity, transfected area and dynamic of expression obtained in the muscle (Fig. 2) after the combined treatment of HI-PEMF and injection of pEGFP-N1 (HI-PEMF + EGFP) were comparable to the treatment with conventional electroporation (EP + EGFP). Whereas in the skin, higher fluorescence intensity and larger areas were determined with HI-PEMF compared to conventional electroporation (Fig. 3B,C). The expression of EGFP was obtained in deeper skin layers, with a maximal peak at day 7, thereafter started to decline reaching the plato (lasted to 80 days) and afterwards between 80 and 90 days started to blur in most cases or even disappear in some cases (Fig. 3). Furthermore, the expression of EGFP was determined also in the upper layer of skin (Fig. 4), which started to blur after one and disappear after two weeks. In both, muscle and in the skin, the highest fluorescence intensity was detected in areas that were closest to the surface of the applicator, i.e., where the induced electric field was the highest.

3.2. Histological analysis after gene electrotransfer in muscle tibialis cranialis

As can be observed in Fig. 5, 48 h after the application of either high intensity pulsed electromagnetic field (HI-PEMF), conventional electroporation (EP), injection of pEGFP-N1 plasmid (pEGFP), injection of pEGFP-N1 and application of HI-PEMF (HI-PEMF + pEGFP) or injection of pEGFP-N1 and application of conventional electroporation (EP + pEGFP) the inflammatory infiltrate was diffusely distributed in the endomysium around the muscle fibers. Lymphocytes and plasma cells dominating among inflammatory cells. Combined treatment of plasmid injection and application of conventional electric pulses resulted in a significant increase in inflammatory mononuclear cells up to 38% of muscle area. Interestingly, combined treatment of plasmid injection with the application of HI-PEMF induced the infiltration of inflammatory mononuclear cells up to 15% of muscle area. There was no inflammatory immune cell infiltration after HI-PEMF application or conventional application using electric pulses and contact electrodes alone.

3.3. Antitumor effect of silencing MCAM mediated by HI-PEMF

As a model for evaluating and comparing the antitumor effect of silencing MCAM mediated by HI-PEMF to conventional electroporation, a B16F10 melanoma was used that has previously shown the therapeutic potential of MCAM silencing [9]. Silencing MCAM using HI-PEMF delayed tumor growth (up to 5 days compared to control) with no tumor cures observed (Table 1, Fig. 6,). The antitumor effect was also observed after electrotransfer of nontherapeutic plasmid mediated by HI-PEMF but was less evident compared to the therapeutic plasmid, resulted in a 3.6 days shorter tumor growth delay. The most pronounced antitumor effect of therapeutic and nontherapeutic plasmid DNA was observed after using conventional electroporation for GET (GET pMCAM, GET pControl). Silencing MCAM using conventional GET (GET pMCAM) significantly delayed tumor growth compared to all other groups (control, monotherapies, GET pControl, and groups where electrotransfer of a therapeutic and nontherapeutic gene was mediated by HI-PEMF) (Table 1, Fig. 6). In addition, silencing of MCAM using conventional GET therapy cured 37,5% of tumors and 66.7% of these mice were resistant to secondary challenge (Tumor growth curves of mice that were not resistant to secondary challenge are available in Supplementary material). A similar but significantly lower antitumor effect was determined after electrotransfer of plasmid DNA encoding of a non-therapeutic gene by conventional electroporation (GET pControl), which resulted in

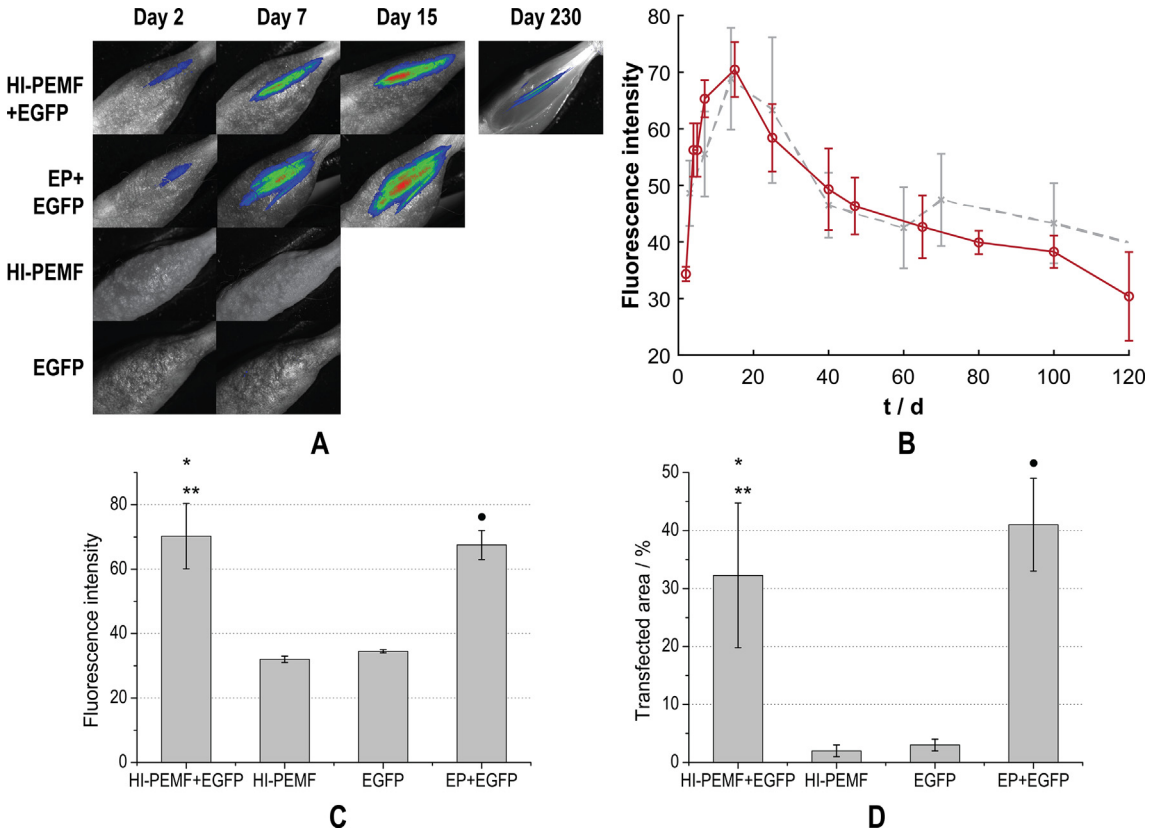

Fig. 2. *In vivo* plasmid EGFP in *tibialis cranialis* muscle in SKH1-Elite mice. (**A**) Representative images of EGFP fluorescence in a muscle at different time points. (**B**) Time course of fluorescence intensity after the treatment of either HI-PEMF + EGFP (red solid line) or EP + EGFP (grey dashed line). Each point represents mean and standard error of the mean. (**C**) The quantification of the intensity of EGFP fluorescence in excised muscles 5 days after the treatment. Data represents mean and standard error of the mean. (**D**) Percentage of the transfected area in excised muscles 5 days after the treatment. Data represents mean and standard error of the mean. *: P-value < 0.05; significantly different from HI-PEMF. **: P-value < 0.05; significantly different from EGFP. ●: No statistical difference from HI-PEMF + EGFP; One-way ANOVA.

6.6 days shorter tumor growth delay compared to the group treatead with EP only (EP) and 25% of tumor cures, but none of them were resistant to secondary challenge.

4. Discussion

In our study we demonstrated the use of contactless high intensity pulsed electromagnetic field (HI-PEMF) treatment as a feasible noninvasive approach to achieve *in vivo* transfection by enabling the transport of larger molecules such as plasmid DNA encoding EGFP into muscle and skin. Furthermore, the antitumor effectiveness using HI-PEMF for electrotransfer of therapeutic plasmid, i.e., silencing MCAM was demonstrated. HI-PEMF treatment may thus represent an important tool in research and clinical applications for noninvasive gene/nucleic acid delivery *in vivo* since HI-PEMF is easy to perform, is non-invasive, contactless, and painless.

Generally two target tissues, muscle and skin, were shown as interesting in gene manipulation [27,34,37-40]. The specific biological characteristics of skeletal muscle, i.e., high capacity of protein synthesis, postmitotic nature, the longevity of muscle fibers, the presence of muscle precursor cells enable long-lasting transgene expression either locally or systemically, thus makes it as promising approach in gene therapy [17,21,23,40]. Muscle gene transfection has been tested in the treatment of muscular disorder, local secretion of angiogenic and neurotrophic factors and systemic secretion of therapeutic proteins such as erythropoietin, coagulation factors and anti-inflammatory cytokines [38,39]. Another tissue attractive for gene therapy and vaccination is skin. Specifically, the skin complexity, different layers consisted of different cell types, enable the long term expression in transfected muscle cells (rarely divide), short term in transfected keratinocytes (fast dividing cell), also in deeper layers of skin [34,37,41-43], which could altogether affect on the localization and expression of transgene.

The delivery of foreign material to the target tissue (skeletal muscle, skin, tumor) is crucial for the effective expression of the transgene. Gene transfer of different molecules using conventional electroporation was shown to be an attractive and efficient approach for gene therapy in a variety of normal tissues (muscle, skin) and tumor, as well as for DNA vaccination in preclinical and clinical studies [26,31,44-55]. Depending on the targeted molecule or specific gene (K-ras, CD105, MCAM, IL-12, AMEP, erithropoetin, p53, CpG or GpC oligonucleotides, bacterial purine nucleoside phosphorylase (ePNP)) [31,45,46,49,51,53,56-59], good antitumor, antimetastatic and/or vascular targeted effects were demonstrated. Although conventional electroporation, i.e., electric pulse-mediated electrotransfer, is inexpensive and simple, it has several limitations and disadvantages, such as the narrow range of clinically safe electric field parameters, the possible undesired tissue damage by irreversible electroporation, and the mandatory contact of electrodes with the tissue [29,60,61].

We have shown previouly that small molecules can be delivered into cells with HI-PEMF *in vitro* [8] and *in vivo* [9,10]. In this study, we obtained a long term expression of EGFP in the muscle and skin after HI-PEMF and conventional electroporation, in some mice even up to 230 days (Fig. 2a) and up to 190 days (Fig. 3a), respectively. The results are in agreement with the studies where

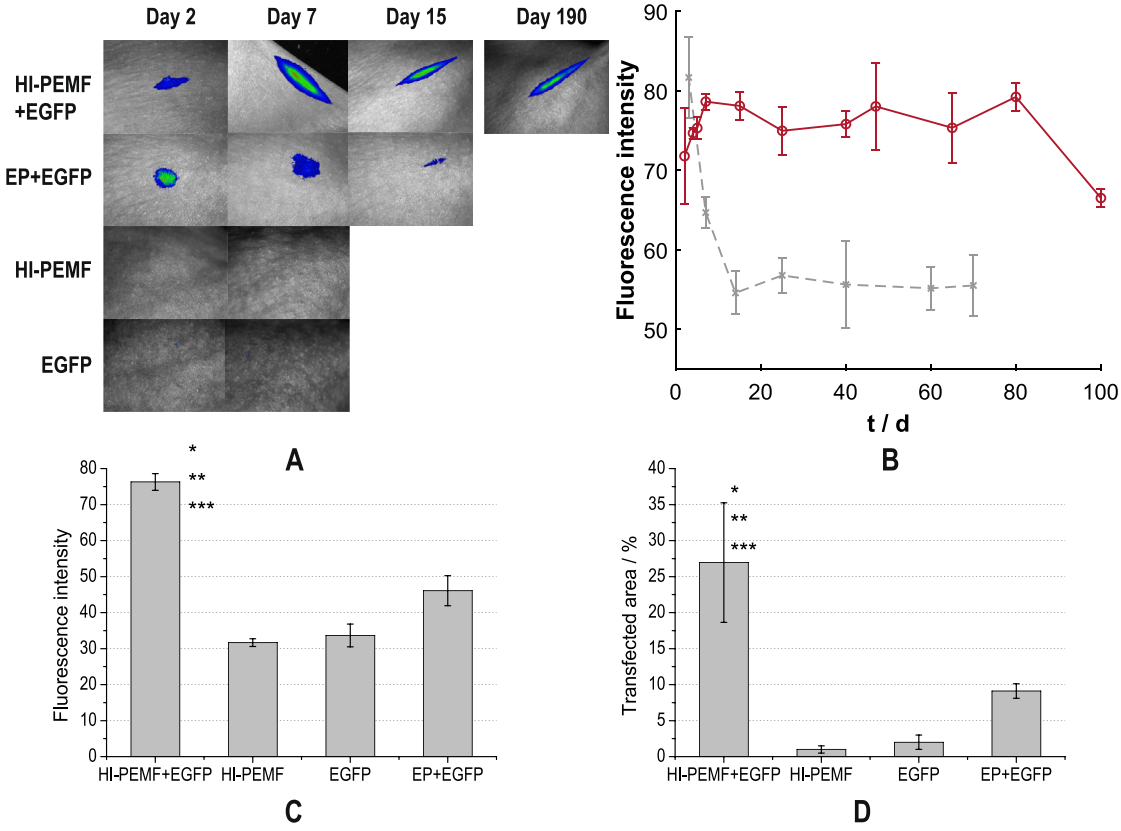

Fig. 3. *In vivo* plasmid EGFP electrotransfer in the skin in SKH1-Elite mice. (**A**) Representative images of EGFP fluorescence in the skin at different time points. (**B**) Time course of fluorescence intensity after the treatment of either HI-PEMF + EGFP (red solid line) or EP + EGFP (grey dashed line). Each point represents mean and standard error of the mean. (**C**) The quantification of the intensity of EGFP fluorescence in the skin 5 days after the treatment. Data represents mean and standard error of the mean. (**D**) Percentage of the transfected area in skin 5 days after the treatment. Data represents mean and standard error of the mean. *: P-value < 0.05; significantly different from HI-PEMF. **: P-value < 0.05; significantly different from EGFP. ***: P-value < 0.05; significantly different from EP + EGFP; One-way ANOVA.

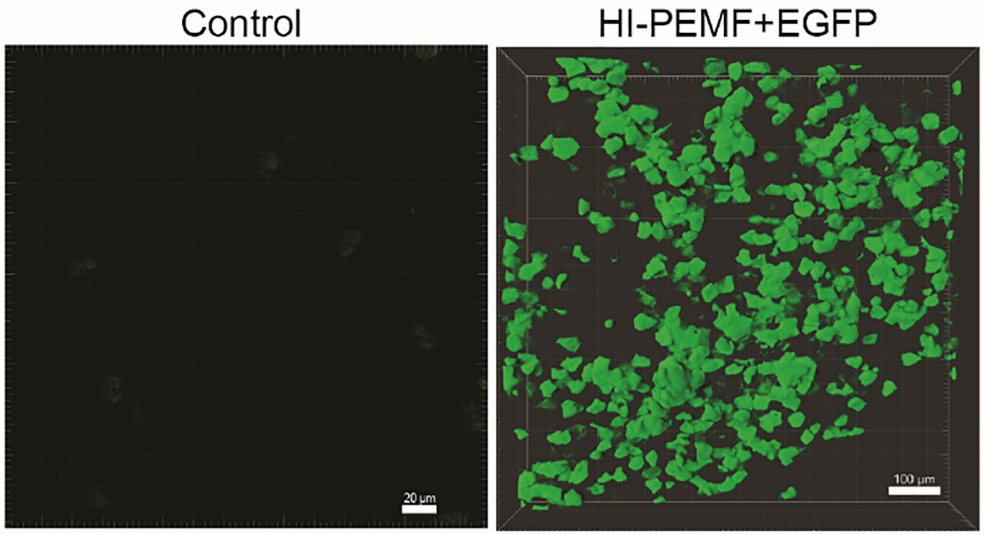

Fig. 4. The expression of enhanced green fluorescent protein (EGFP) in upper skin layer after using high-intensity magnetic fields (HI-PEMF) at day 2 post-transfection. The image represents three views of skin from the top, bottom, and from the side of imaged area of skin in 152 µm thickness. A 3D view of cells in skin was obtained using the Imaris software suite (Bitplane, Zurich, Switzerland). White bar in the left image represent 20 µm and in the right image represent 100 µm length.

long-term expression up to 18 months using conventional electroporation was reported [21,27,62]. Besides, Tevz et al determined 25% of the transfected area of the whole muscle after electrotransfer of 30 µg of plasmid DNA encoding EGFP at day 7 post-transfection. Similarly in our study around 30% of the transfected muscle area was obtained at day 5 post-transfection (Fig. 2d). Furthermore, HI-PEMF was tested for transfection in skin tissue. The obtained transfected area in the skin using HI-PEMF was significantly higher, up to 3-fold compared to conventional electroporation (Fig. 3d). Targeting different types of cells with different

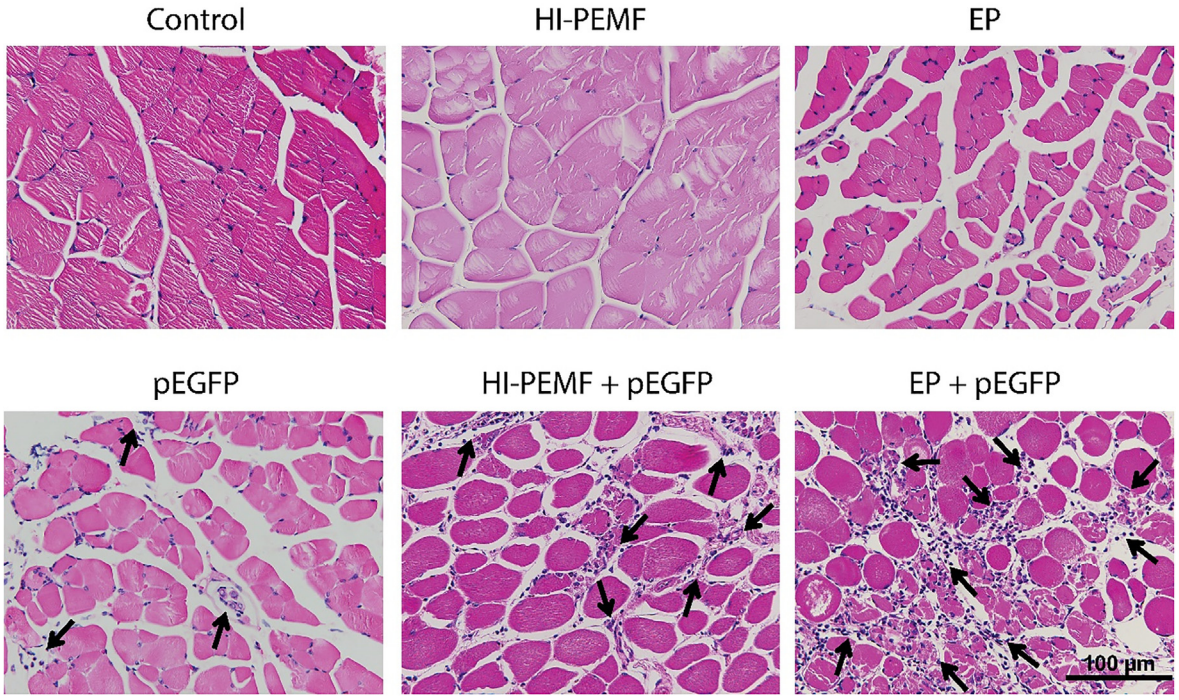

Fig. 5. Histological analysis 48 h after electrotransfer of EGFP transfected by HI-PEMF and conventional EP. Black arrows show the area of infiltration of inflammatory mononuclear cells. HI-PEMF: application of high intensity pulsed electromagnetic field; EP: conventional electroporation (1 × HV + 4 × LV electric pulses); pEGFP: injection of pEGFP-N1 plasmid; HI-PEMF + pEGFP: injection of pEGFP-N1 and application of HI-PEMF; EP + pEGFP: injection of pEGFP-N1 combined with conventional electroporation (1 × HV + 4 × LV electric pulses).

Table 1
Tumor growth delay after gene electrotransfer of plasmid DNA encoding shRNA against MCAM in melanoma B16F10.

Group	N	DT (days)	SE	GD (days)	CR (n, %)	SC (n, %)
Control	6	1.2	0.1		0	/
EP conventional	6	2.6	0.4	1.4	0	/
HI-PEMF	6	1.4	0.1	0.2	0	/
pMCAM	6	1.6	0.1	0.4	0	/
pControl	6	1.5	0.2	0.3	0	/
GET pMCAM	8	15.7*	2.1	14.5	3 (37.5)	2 (66.7)
HI-PEMF pMCAM	8	6.8	0.3	5.6	0	/
GET pControl	8	9.3**	3.6	8.1	2 (25.0)	/
HI-PEMF pControl	8	3.3	0.2	2.1	0	/

N- number of animals in a group; DT- tumor doubling time; SE- standard error; GD- tumor growth delay compared to control; CR- complete response; SC- secondary challenge; EP- application of electric pulses; HI-PEMF- application of high-intensity of pulsed electromagnetic fields; pMCAM- intratumorally injection of plasmid DNA encoding shRNA against MCAM; pControl- intratumorally injection of control plasmid; GET- conventional gene electrotransfer; *P < 0.05 significant to HI-PEMF pMCAM, GET pControl, HI-PEMF pControl; **P < 0.05 significant to HI-PEMF pControl; One-way ANOVA.

turnover in skin layers resulted in different duration of transgene expression; i.e. long-term in muscle cells and short-term in keratinocytes [41,63]. In a previous study using multi-electrode array electroporation it was reported that by using different pulse parameters gene expression in the skin can be controlled; the high-voltage electric pulses for superficial expression of the transgene which enabled a local response; and the low-voltage electric pulses in the deeper skin layers (muscle layers *Panninculus carnosus* below the dermis), which enable the prolonged gene expression and higher transgene production, possibly with systemic distribution [34]. Interestingly, in our study we observed transfection of both, in the upper layers (keratinocytes) and the deeper layers (including muscle) of the skin using HI-PEMF. Visually detected transfection started to blur after 80–90 days, thus we presume that the transfection of muscle Panniculus carnosus was observed, which has longer turn over compared to cells in the epidermis and dermis. Thus, HI-PEMF as gene delivery method could be used in vaccination, where local immune response of the skin cell is expected, as well for the muscle transfection used for delivery of molecules with systemic action. Therefore, in the translation into the clinics, it will be important to evaluate the level and duration of transgene expression after using HI-PEMF.

As a proof of principle, the HI-PEMF as a delivery method was further tested in antitumor effectiveness of plasmid encoding MCAM (therapeutic plasmid) in B16F10 immunologically responsive melanoma and compared to conventional gene electrotransfer. Recently it has been shown that conventional gene electrotransfer of pMCAM in B16F10 melanoma, significantly delayed tumor growth (up to 13 days compared to control) and cured 36% of mice, of which 60% were resistant to secondary challenge [35]. Similarly, the antitumor effect was confirmed with GET of nontherapeutic control plasmid (pControl); the tumor growth delays up to 10 days, 31% of cured tumor of which 20% were resistant to secondary challenge. The results from that and other studies indicated the induction of immune response after GET of therapeutic and nontherapeutic plasmids [32,35,64-66]. In the same tumor model,

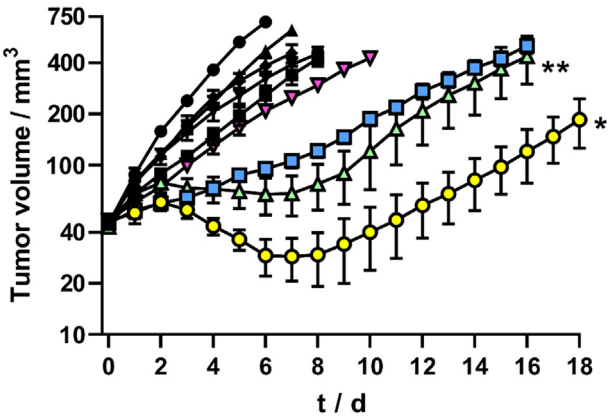

Fig. 6. Growth curves of B16F10 melanoma tumors after treatment with gene electrotransfer of plasmid DNA encoded shRNA against MCAM (pMCAM) mediated by HI-PEMF or conventional electroporation (GET). Each therapy was performed three times (on day 0, day 2 and day 4). The data represent the arithmetic mean and standard error of the mean, n = 6–8; *P < 0.05 significant to HI-PEMF pMCAM; **P < 0.05 significant to HI-PEMF pControl; One-way ANOVA; black circles – control; black squares - EP; black triangles - HI-PEMF; black upside down triangles – pMCAM; black diamonds – pControl; yellow circles – GET pMCAM (2 CR); blue squares – HI-PEMF pMCAM; green triangles – GET pControl (1 CR); violet upside down triangles – HI-PEMF pControl.

Marrero *et al* [65] obtained up to 71% of animals that were resistant to the secondary challenge after GET of control pVaX1 plasmid, while in the studies of Savarin *et al* [32] and Kranjc Brezar *et al* [35], they determined up to 100% of animals that were resistant to the secondary challenge after GET of pControl. Similar results were obtained also in our study after conventional gene electrotransfer of pMCAM or pControl. In the case of GET pMCAM 37.5% of tumors were cured and 66.7% of them were resistant to secondary challenge. A less pronounced effect was observed after GET pControl treatment resulting in 25% of tumor cures and no resistance to secondary challenge (Table 1). The antitumor effect after using HI-PEMF to deliver therapeutic and nontherapeutic plasmids in melanoma was less evident. The growth of tumors after HI-PEMF pMCAM was delayed significantly less (for 8.9 days) compared to conventional gene electrotransfer and no tumor cures were observed (Table 1, Fig. 6) and insignificantly less compared to GET pControl. Nevertheless, tumor growth was still significantly delayed (up to 5.6 days) compared to all other pertinent control groups (Control, either of therapeutic or nontherapeutic plasmid injection only, HI-PEMF, HI-PEMF pControl).

It was reported in several studies that electroporation as a delivery method of plasmid DNA or other molecules induces local tissue damage and lymphocyte infiltration [27]. The infiltration of mononuclear cells after the injection of plasmid DNA or GET combined with the injection of plasmid DNA determined 48 h after the treatment reached up to 30% and 60% of muscle area, respectively. Similarly, we observed a significant increase of 38% in inflammatory mononuclear cells of muscle area after conventional gene electrotransfer of pEGFP compared to control. However, the delivery of pEGFP using HI-PEMF induced significantly less infiltration of inflammatory mononuclear cells compared to conventional gene electrotransfer (Fig. 5). In controlling of systemic action of expressed proteins, HI-PEMF induced no tissue damage and less mononuclear cell infiltration compared to conventional electroporation.

Although nonviral delivery of genetic material into cells using conventional electroporation holds great promise for basic research and clinics, it has some limitations, i.e., low transfection efficiency compared to other methods [67-70], presence of electrochemical reactions, alteration of pH [28-30] and difficulties in controlling the delivery due to an incomplete understanding of its mechanisms [71-74]. In the gene electrotransfer using conventional electroporation of cells and tissues, it is postulated that plasmid DNA can enter through pores only partially. Mainly clathrin-mediated or Rac-1-dependent endocytosis processes are then responsible for the transport of plasmid DNA across the membrane and cytoplasm to the nucleus [73-76]. Such processes demand optimized electric pulse parameters, i.e., longer, high voltage or a combination of short, high voltage and long, low voltage pulses [27,71,76-82]. Furthermore, the alterations in the pH of the medium during electroporation may cause denaturation of the plasmid DNA or reduces pDNA uptake and thus plays an important role in DNA electrotransfer [28,29]. Additionally, the temperature affects the cell membrane fluidity and consequently, its electroporation [83]. It was shown that gene electrotransfer could be thermally assisted. Specifically, heating applied before electroporation enabled a similar level of transfection efficiency in skin using an approximately 30% lower electric field [84]. In our study, we observed an increase in the temperature of the magnetic coil (to approximately 40 °C, data not shown), and we assume that some transfer of heat could have led to a thermal effect in the tissue during electroporation, thus affecting the transfection efficiency in the skin but this is not a case in muscle and tumor due to slow thermal diffusion in tissue. Besides, the heterogeneity of tissue, i.e., the cell type organization and extracellular matrix composition, has a substantial impact on transfection efficiency. It was shown that modification of the tissue extracellular matrix improved the transfection efficiency, due to a better plasmid DNA distribution within the tissue [79,85]. In summary, we are aware of all these factors that might have affected the transfection efficiency in the present study and intend to address this possibility in a further study, both by optimizing the conditions of HI-PEMF and improving the equipment, i.e., the coil and magnetic pulse generator. Our long-term goal is to develop the devices and applicators for noninvasive noncontact electroporation and mechanistic knowledge that will allow further optimization of the device, applicators and gene transfer protocols and by this development of gene therapies, which will be safer and also more accessible.

5. Conclusion

In conclusion, our results show that a high-intensity pulsed electromagnetic fields (HI-PEMF) at a time-varying magnetic field below 1 T are capable of a facilitating delivery of large molecules of plasmid DNA (pEGFP-N1) in different tissues (muscle, skin and tumors). Furthermore, the antitumor effectiveness using HI-PEMF for electrotransfer of therapeutic plasmid pMCAM was demonstrated. Due to the potential and contactless application of HI-PEMF, this approach represents for gene therapy and DNA vaccination a viable alternative to conventional electroporation. Further studies are warranted to improve the equipment, HI-PEMF parameters and to optimize the protocols for gene transfection.

Disclosure

Funding: Authors acknowledge the financial support of the Slovenian Research Agency (research core funding No. P2-0249, No. P3-0003, J2-1733 to MK and J2-9225 to DM). This study was conducted within Infrastructure Programme: Network of research infrastructure centers at the University of Ljubljana (MRIC UL IP-0510).

CRediT authorship contribution statement

Matej Kranjc: Methodology, Investigation, Formal analysis, Visualization. **Simona Kranjc Brezar:** Methodology, Investigation, Formal analysis, Visualization. **Gregor Serša:** Methodology,

Resources, Supervision, Project administration, Funding acquisition. **Damijan Miklavčič:** Conceptualization, Methodology, Resources, Supervision, Project administration, Funding acquisition.

Declaration of Competing Interest

The authors declare that they have no known competing financial interests or personal relationships that could have appeared to influence the work reported in this paper.

Appendix A. Supplementary data

Supplementary data to this article can be found online at https://doi.org/10.1016/j.bioelechem.2021.107847.

References

[1] M.-O. Mattsson, M. Simkó, Emerging medical applications based on non-ionizing electromagnetic fields from 0 Hz to 10 THz, Med. Devices Evid. Res. 12 (2019) 347–368, https://doi.org/10.2147/MDER.S214152.

[2] C. Andrew, L. Bassett, R.J. Pawluk, A.A. Pilla, Augmentation of Bone Repair by Inductively Coupled Electromagnetic Fields, Science (80-.). 184 (1974) 575–577, https://doi.org/10.1126/science.184.4136.575.

[3] A. Streit, B.C. Watson, J.D. Granata, T.M. Philbin, H.-N. Lin, J.P. O'Connor, S. Lin, Effect on Clinical Outcome and Growth Factor Synthesis With Adjunctive Use of Pulsed Electromagnetic Fields for Fifth Metatarsal Nonunion Fracture, Foot Ankle Int. 37 (2016) 919–923, https://doi.org/10.1177/1071100716652621.

[4] R.J. Ilmoniemi, J. Ruohonen, J. Karhu, Transcranial magnetic stimulation–a new tool for functional imaging of the brain., Crit. Rev. Biomed. Eng. 27 (1999) 241–84. http://www.ncbi.nlm.nih.gov/pubmed/10864281.

[5] A.T. Barker, R. Jalinous, I.L. Freeston, Non-Invasive Magnetic Stimulation of Human Motor Cortex, Lancet. 325 (1985) 1106–1107, https://doi.org/10.1016/S0140-6736(85)92413-4.

[6] M. Hallett, Transcranial magnetic stimulation and the human brain, Nature. 406 (2000) 147–150, https://doi.org/10.1038/35018000.

[7] M.C. Ridding, J.C. Rothwell, Is there a future for therapeutic use of transcranial magnetic stimulation?, Nat. Rev. Neurosci. 8 (2007) 559–567, https://doi.org/10.1038/nrn2169.

[8] V. Novickij, J. Dermol, A. Grainys, M. Kranjc, D. Miklavčič, Membrane permeabilization of mammalian cells using bursts of high magnetic field pulses, PeerJ. 5 (2017), https://doi.org/10.7717/peerj.3267 e3267.

[9] S. Kranjc Brezar, M. Kranjc, M. Čemažar, S. Buček, G. Serša, D. Miklavčič, Electrotransfer of siRNA to Silence Enhanced Green Fluorescent Protein in Tumor Mediated by a High Intensity Pulsed Electromagnetic Field, Vaccines. 8 (2020) 49, https://doi.org/10.3390/vaccines8010049.

[10] S. Kranjc, M. Kranjc, J. Scancar, J. Jelenc, G. Sersa, D. Miklavcic, Electrochemotherapy by pulsed electromagnetic field treatment (PEMF) in mouse melanoma B16F10 in vivo, Radiol. Oncol. 50 (2016) 39–48, https://doi.org/10.1515/raon-2016-0014.

[11] L. Towhidi, S.M.P. Firoozabadi, H. Mozdarani, D. Miklavcic, Lucifer Yellow uptake by CHO cells exposed to magnetic and electric pulses, Radiol. Oncol. 46 (2012) 119–125, https://doi.org/10.2478/v10019-012-0014-2.

[12] V. Novickij, A. Grainys, I. Kucinskaite-Kodze, A. Zvirbliene, J. Novickij, Magneto-Permeabilization of Viable Cell Membrane Using High Pulsed Magnetic Field, IEEE Trans. Magn. 51 (2015) 1–5, https://doi.org/10.1109/TMAG.2015.2439638.

[13] T. Kotnik, L. Rems, M. Tarek, D. Miklavčič, Membrane Electroporation and Electropermeabilization: Mechanisms and Models, Annu. Rev. Biophys. 48 (2019) 63–91, https://doi.org/10.1146/annurev-biophys-052118-115451.

[14] K. Tatiparti, S. Sau, S. Kashaw, A. Iyer, siRNA Delivery Strategies: A Comprehensive Review of Recent Developments, Nanomaterials. 7 (2017) 77, https://doi.org/10.3390/nano7040077.

[15] B. Hu, L. Zhong, Y. Weng, L. Peng, Y. Huang, Y. Zhao, X.-J. Liang, Therapeutic siRNA: state of the art, Signal Transduct. Target. Ther. 5 (2020) 101, https://doi.org/10.1038/s41392-020-0207-x.

[16] C. Scholz, E. Wagner, Therapeutic plasmid DNA versus siRNA delivery: Common and different tasks for synthetic carriers, J. Control. Release. 161 (2012) 554–565, https://doi.org/10.1016/j.jconrel.2011.11.014.

[17] J.A. Wolff, R.W. Malone, P. Williams, W. Chong, G. Acsadi, A. Jani, P.L. Felgner, Direct gene transfer into mouse muscle in vivo, Science. 247 (1990) 1465–1468, https://doi.org/10.1126/science.1690918.

[18] T. Niidome, L. Huang, Gene therapy progress and prospects: nonviral vectors, Gene Ther. 9 (2002) 1647–1652, https://doi.org/10.1038/sj.gt.3301923.

[19] H. Yin, R.L. Kanasty, A.A. Eltoukhy, A.J. Vegas, J.R. Dorkin, D.G. Anderson, Non-viral vectors for gene-based therapy, Nat. Rev. Genet. 15 (2014) 541–555, https://doi.org/10.1038/nrg3763.

[20] D.J. Wells, Gene Therapy Progress and Prospects: Electroporation and other physical methods, Gene Ther. 11 (2004) 1363–1369, https://doi.org/10.1038/sj.gt.3302337.

[21] L.M. Mir, M.F. Bureau, J. Gehl, R. Rangara, D. Rouy, J.M. Caillaud, P. Delaere, D. Branellec, B. Schwartz, D. Scherman, High-efficiency gene transfer into skeletal muscle mediated by electric pulses, Proc. Natl. Acad. Sci. U. S. A. 96 (1999) 4262–4267, https://doi.org/10.1073/pnas.96.8.4262.

[22] G. Rizzuto, M. Cappelletti, D. Maione, R. Savino, D. Lazzaro, P. Costa, I. Mathiesen, R. Cortese, G. Ciliberto, R. Laufer, N. La Monica, E. Fattori, Efficient and regulated erythropoietin production by naked DNA injection and muscle electroporation, Proc. Natl. Acad. Sci. U. S. A. 96 (1999) 6417–6422, https://doi.org/10.1073/pnas.96.11.6417.

[23] H. Aihara, J. Miyazaki, Gene transfer into muscle by electroporation in vivo, Nat. Biotechnol. 16 (1998) 867–870, https://doi.org/10.1038/nbt0998-867.

[24] I. Mathiesen, Electropermeabilization of skeletal muscle enhances gene transfer in vivo, Gene Ther. 6 (1999) 508–514, https://doi.org/10.1038/sj.gt.3300847.

[25] P. Chiarella, E. Massi, M. De Robertis, E. Signori, V.M. Fazio, Adjuvants in vaccines and for immunisation: Current trends, Expert Opin. Biol. Ther. 7 (2007) 1551–1562, https://doi.org/10.1517/14712598.7.10.1551.

[26] L. Lambricht, A. Lopes, S. Kos, G. Sersa, V. Préat, G. Vandermeulen, Clinical potential of electroporation for gene therapy and DNA vaccine delivery, Expert Opin. Drug Deliv. 13 (2016) 295–310, https://doi.org/10.1517/17425247.2016.1121990.

[27] G. Tevz, D. Pavlin, U. Kamensek, S. Kranjc, S. Mesojednik, A. Coer, G. Sersa, M. Cemazar, Gene electrotransfer into murine skeletal muscle: A systematic analysis of parameters for long-term gene expression, Technol. Cancer Res. Treat. 7 (2008) 91–101, https://doi.org/10.1177/153303460800700201.

[28] T. Potočnik, D. Miklavčič, A. Maček Lebar, Effect of electroporation and recovery medium pH on cell membrane permeabilization, cell survival and gene transfer efficiency in vitro, Bioelectrochemistry. 130 (2019), https://doi.org/10.1016/j.bioelechem.2019.107342 107342.

[29] P. Turjanski, N. Olaiz, F. Maglietti, S. Michinski, C. Suárez, F.V. Molina, G. Marshall, The role of pH fronts in reversible electroporation, PLoS One. 6 (2011), https://doi.org/10.1371/journal.pone.0017303.

[30] S. Mahnič-Kalamiza, D. Miklavčič, Scratching the electrode surface: Insights into a high-voltage pulsed-field application from in vitro & in silico studies in indifferent fluid, Electrochim. Acta. 363 (2020), https://doi.org/10.1016/j.electacta.2020.137187 137187.

[31] L. Prosen, B. Markelc, T. Dolinsek, B. Music, M. Cemazar, G. Sersa, Mcam silencing with RNA interference using magnetofection has antitumor effect in murine melanoma, Mol. Ther. - Nucleic Acids. 3 (2014), https://doi.org/10.1038/mtna.2014.56 e205.

[32] M. Savarin, U. Kamensek, M. Cemazar, R. Heller, G. Sersa, Electrotransfer of plasmid DNA radiosensitizes B16F10 tumors through activation of immune response, Radiol. Oncol. 51 (2017) 30–39, https://doi.org/10.1515/raon-2017-0011.

[33] B.J. Roth, L.G. Cohen, M. Hallett, W. Friauf, P.J. Basser, A theoretical calculation of the electric field induced by magnetic stimulation of a peripheral nerve, Muscle Nerve. 13 (1990) 734–741, https://doi.org/10.1002/mus.880130812.

[34] S. Kos, T. Blagus, M. Cemazar, U. Lampreht Tratar, M. Stimac, L. Prosen, T. Dolinsek, U. Kamensek, S. Kranjc, L. Steinstraesser, G. Vandermeulen, V. Préat, G. Sersa, Electrotransfer parameters as a tool for controlled and targeted gene expression in skin, Mol. Ther. - Nucleic Acids. 5 (2016), https://doi.org/10.1038/mtna.2016.65 e356.

[35] S. Kranjc Brezar, V. Mrak, M. Bosnjak, M. Savarin, G. Sersa, M. Cemazar, Intratumoral Gene Electrotransfer of Plasmid DNA Encoding shRNA against Melanoma Cell Adhesion Molecule Radiosensitizes Tumors by Antivascular Effects and Activation of an Immune Response, Vaccines. 8 (2020) 135, https://doi.org/10.3390/vaccines8010135.

[36] J. Schindelin, I. Arganda-Carreras, E. Frise, V. Kaynig, M. Longair, T. Pietzsch, S. Preibisch, C. Rueden, S. Saalfeld, B. Schmid, J.-Y. Tinevez, D.J. White, V. Hartenstein, K. Eliceiri, P. Tomancak, A. Cardona, Fiji: an open-source platform for biological-image analysis, Nat. Methods. 9 (2012) 676–682, https://doi.org/10.1038/nmeth.2019.

[37] P.A. Gerber, B.A. Buhren, H. Schrumpf, B. Homey, A. Zlotnik, P. Hevezi, The top skin-associated genes: a comparative analysis of human and mouse skin transcriptomes, Biol. Chem. 395 (2014) 577–591, https://doi.org/10.1515/hsz-2013-0279.

[38] J. Vilquin, P. Kennel, M. Paturneau-Jouas, P. Chapdelaine, N. Boissel, P. Delaère, J. Tremblay, D. Scherman, M. Fiszman, K. Schwartz, Electrotransfer of naked DNA in the skeletal muscles of animal models of muscular dystrophies, Gene Ther. 8 (2001) 1097–1107, https://doi.org/10.1038/sj.gt.3301484.

[39] T. Ragot, N. Vincent, P. Chafey, E. Vigne, H. Gilgenkrantz, D. Coutont, J. Cartaud, P. Briand, J.-C. Kaplant, M. Perricaude, A. Kahn, Efficient adenovirus-mediated transfer of a human minidystrophin gene to skeletal muscle of mdx mice, Nature. 361 (1993) 647–650, https://doi.org/10.1038/361647a0.

[40] Q.L. Lu, G. Bou-Gharios, T.A. Partridge, Non-viral gene delivery in skeletal muscle: a protein factory, Gene Ther. 10 (2003) 131–142, https://doi.org/10.1038/sj.gt.3301874.

[41] A. Gothelf, J. Gehl, Gene Electrotransfer to Skin; Review of Existing Literature and Clinical Perspectives, Curr. Gene Ther. 10 (2010) 287–299, https://doi.org/10.2174/156652310791823443.

[42] T. Blagus, B. Markelc, M. Cemazar, T. Kosjek, V. Preat, D. Miklavcic, G. Sersa, In vivo real-time monitoring system of electroporation mediated control of transdermal and topical drug delivery, J. Control. Release. 172 (2013) 862–871, https://doi.org/10.1016/j.jconrel.2013.09.030.

[43] N. Naldaiz-Gastesi, M. Goicoechea, S. Alonso-Martín, A. Aiastui, M. López-Mayorga, P. García-Belda, J. Lacalle, C. San José, M.J. Araúzo-Bravo, L. Trouilh, V.

Anton-Leberre, D. Herrero, A. Matheu, A. Bernad, J.M. García-Verdugo, J.J. Carvajal, F. Relaix, A. Lopez de Munain, P. García-Parra, A. Izeta, Identification and Characterization of the Dermal Panniculus Carnosus Muscle Stem Cells, Stem Cell Reports. 7 (2016) 411–424, https://doi.org/10.1016/j.stemcr.2016.08.002.
[44] M. Golzio, L. Mazzolini, A. Ledoux, A. Paganin, M. Izard, L. Hellaudais, A. Bieth, M.J. Pillaire, C. Cazaux, J.S. Hoffmann, B. Couderc, J. Teissié, In vivo gene silencing in solid tumors by targeted electrically mediated siRNA delivery, Gene Ther. 14 (2007) 752–759, https://doi.org/10.1038/sj.gt.3302920.
[45] T. Dolinsek, B. Markelc, G. Sersa, A. Coer, M. Stimac, J. Lavrencak, A. Brozic, S. Kranjc, M. Cemazar, Multiple delivery of siRNA against endoglin into murine mammary adenocarcinoma prevents angiogenesis and delays tumor growth, PLoS One. 8 (2013), https://doi.org/10.1371/journal.pone.0058723 e58723.
[46] M. Bosnjak, T. Dolinsek, M. Cemazar, S. Kranjc, T. Blagus, B. Markelc, M. Stimac, J. Zavrsnik, U. Kamensek, L. Heller, C. Bouquet, B. Turk, G. Sersa, Gene electrotransfer of plasmid AMEP, an integrin-targeted therapy, has antitumor and antiangiogenic action in murine B16 melanoma, Gene Ther. 22 (2015) 578–590, https://doi.org/10.1038/gt.2015.26.
[47] N. Tesic, U. Kamensek, G. Sersa, S. Kranjc, M. Stimac, U. Lampreht, V. Preat, G. Vandermeulen, M. Butinar, B. Turk, M. Cemazar, Endoglin (CD105) silencing mediated by shRNA under the control of endothelin-1 promoter for targeted gene therapy of melanoma, Mol. Ther. - Nucleic Acids. 4 (2015), https://doi.org/10.1038/mtna.2015.12.
[48] I. Spanggaard, M. Snoj, A. Cavalcanti, C. Bouquet, G. Sersa, C. Robert, M. Cemazar, E. Dam, B. Vasseur, P. Attali, L.M. Mir, J. Gehl, Gene electrotransfer of plasmid antiangiogenic metargidin peptide (AMEP) in disseminated melanoma: Safety and efficacy results of a phase i first-in-man study, Hum. Gene Ther. Clin. Dev. 24 (2013) 99–107, https://doi.org/10.1089/humc.2012.240.
[49] R. Heller, L.C. Heller, Gene Electrotransfer Clinical Trials, Adv. Genet. 89 (2015) 235–262, https://doi.org/10.1016/bs.adgen.2014.10.006.
[50] L.C. Heller, R. Heller, Electroporation Gene Therapy Preclinical and Clinical Trials for Melanoma, Curr. Gene Ther. 10 (2010) 312–317, https://doi.org/10.2174/156652310791823489.
[51] L. Heller, V. Todorovic, M. Cemazar, Electrotransfer of single-stranded or double-stranded DNA induces complete regression of palpable B16.F10 mouse melanomas, Cancer Gene Ther. 20 (2013) 695–700, https://doi.org/10.1038/cgt.2013.71.
[52] A. Gothelf, J. Gehl, What you always needed to know about electroporation based DNA vaccines, Hum. Vaccines Immunother. 8 (2012) 1694–1702, https://doi.org/10.4161/hv.22062.
[53] M. Cemazar, T. Jarm, G. Sersa, Cancer Electrogene Therapy with Interleukin-12, Curr. Gene Ther. 10 (2010) 300–311, https://doi.org/10.2174/156652310791823425.
[54] C. Brolin, T. Shiraishi, P. Hojman, T.O. Krag, P.E. Nielsen, J. Gehl, Electroporation Enhanced Effect of Dystrophin Splice Switching PNA Oligomers in Normal and Dystrophic Muscle, Mol. Ther. - Nucleic Acids. 4 (2015), https://doi.org/10.1038/mtna.2015.41 e267.
[55] P. Hojman, C. Brolin, H. Gissel, C. Brandt, B. Zerahn, B.K. Pedersen, J. Gehl, Erythropoietin over-expression protects against diet-induced obesity in mice through increased fat oxidation in muscles, PLoS One. 4 (2009), https://doi.org/10.1371/journal.pone.0005894.
[56] C. Faurie, M. Golzio, P. Moller, J. Teissié, M.-P. Rols, Cell and animal imaging of electrically mediated gene transfer, DNA Cell Biol. 22 (2003) 777–783, https://doi.org/10.1089/104454903322624984.
[57] S. Deharvengt, S. Rejiba, S. Wack, M. Aprahamian, A. Hajri, Efficient electrogene therapy for pancreatic adenocarcinoma treatment using the bacterial purine nucleoside phosphorylase suicide gene with fludarabine, Int. J. Oncol. 30 (2007) 1397–1406.
[58] S. Vidic, B. Markelc, G. Sersa, A. Coer, U. Kamensek, G. Tevz, S. Kranjc, M. Cemazar, MicroRNAs targeting mutant K-ras by electrotransfer inhibit human colorectal adenocarcinoma cell growth in vitro and in vivo, Cancer Gene Ther. 17 (2010) 409–419, https://doi.org/10.1038/cgt.2009.87.
[59] E. Fattori, M. Cappelletti, I. Zampaglione, C. Mennuni, F. Calvaruso, M. Arcuri, G. Rizzuto, P. Costa, G. Perretta, G. Ciliberto, N. La Monica, Gene electro-transfer of an improved erythropoietin plasmid in mice and non-human primates, J. Gene Med. 7 (2005) 228–236, https://doi.org/10.1002/jgm.652.
[60] L. Rubinsky, E. Guenther, P. Mikus, M. Stehling, B. Rubinsky, Electrolytic Effects During Tissue Ablation by Electroporation, Technol. Cancer Res. Treat. 15 (2016) NP95–NP103. https://doi.org/10.1177/1533034615601549.
[61] T. Polajzer, T. Jarm, D. Miklavcic, Analysis of damage-associated molecular pattern molecules due to electroporation of cells in vitro, Radiol. Oncol. 54 (2020) 317–328, https://doi.org/10.2478/raon-2020-0047.
[62] J.M. Vicat, S. Boisseau, P. Jourdes, M. Laine, D. Wion, R. Bouali-Benazzouz, A.L. Benabid, F. Berger, Brief Report: Muscle Transfection by Electroporation with High-Voltage and Short-Pulse Currents Provides High-Level and Long-Lasting Gene Expression, Hum. Gene Ther. 11 (2000) 909–916, https://doi.org/10.1089/10430340050015518.
[63] G. Vandermeulen, E. Staes, M.L. Vanderhaeghen, M.F. Bureau, D. Scherman, V. Préat, Optimisation of intradermal DNA electrotransfer for immunisation, J. Control. Release. 124 (2007) 81–87, https://doi.org/10.1016/j.jconrel.2007.08.010.
[64] T. Dolinsek, G. Sersa, L. Prosen, M. Bosnjak, M. Stimac, U. Razborsek, M. Cemazar, Electrotransfer of plasmid DNA encoding an anti-mouse endoglin (CD105) shRNA to B16 melanoma tumors with low and high metastatic potential results in pronounced anti-tumor effects, Cancers (Basel). 8 (2015), https://doi.org/10.3390/cancers8010003.
[65] Marrero, Delivery of Interleukin-15 to B16 Melanoma by Electroporation Leads to Tumor Regression and Long-term Survival, TCRT Express. (2013). https://doi.org/10.7785/tcrtexpress.2013.600252.
[66] L. Heller, D. Coppola, Electrically mediated delivery of vector plasmid DNA elicits an antitumor effect, Gene Ther. 9 (2002) 1321–1325, https://doi.org/10.1038/sj.gt.3301802.
[67] S.I. Kim, D. Shin, H. Lee, B.Y. Ahn, Y. Yoon, M. Kim, Targeted delivery of siRNA against hepatitis C virus by apolipoprotein A-I-bound cationic liposomes, J Hepatol. 50 (2009) 479–488, https://doi.org/10.1016/j.jhep.2008.10.029.
[68] E.A. Roesch, M.L. Drumm, Powerful tools for genetic modification: Advances in gene editing, Pediatr. Pulmonol. 52 (2017) S15–S20, https://doi.org/10.1002/ppul.23791.
[69] G. Vaseghi, L. Rafiee, S.H. Javanmard, Non-viral Delivery Systems for breast cancer gene therapy, Curr. Gene Ther. (2017), https://doi.org/10.2174/1566523217666170606124131.
[70] R.C. Wilson, L.A. Gilbert, The Promise and Challenge of In Vivo Delivery for Genome Therapeutics, ACS Chem. Biol. 13 (2018) 376–382, https://doi.org/10.1021/acschembio.7b00680.
[71] M. Pavlin, M. Kandušer, New insights into the mechanisms of gene electrotransfer–experimental and theoretical analysis, Sci. Rep. 5 (2015) 9132, https://doi.org/10.1038/srep09132.
[72] M. Wu, F. Yuan, Membrane binding of plasmid DNA and endocytic pathways are involved in electrotransfection of mammalian cells, PLoS One. 6 (2011), https://doi.org/10.1371/journal.pone.0020923.
[73] D.C. Chang, J.A. Saunders, B.M. Chassy, A.E. Sowers, Guide to Electroporation and Electrofusion (2012), https://doi.org/10.1016/C2009-0-21564-9.
[74] M. Mao, L. Wang, C.C. Chang, K.E. Rothenberg, J. Huang, Y. Wang, B.D. Hoffman, P.B. Liton, F. Yuan, Involvement of a Rac1-Dependent Macropinocytosis Pathway in Plasmid DNA Delivery by Electrotransfection, Mol. Ther. 25 (2017) 803–815, https://doi.org/10.1016/j.ymthe.2016.12.009.
[75] J.-M.M. Escoffre, C. Mauroy, T. Portet, L. Wasungu, C. Rosazza, Y. Gilbart, L. Mallet, E. Bellard, M. Golzio, M.-P.P. Rols, J. Teissié, Gene electrotransfer: From biophysical mechanisms to in vivo applications: Part 1- Biophysical mechanisms, Biophys. Rev. 1 (2009) 177–184, https://doi.org/10.1007/s12551-009-0022-7.
[76] C. Faurie, M. Rebersek, M. Golzio, M. Kanduser, J.M. Escoffre, M. Pavlin, J. Teissie, D. Miklavcic, M.P. Rols, Electro-mediated gene transfer and expression are controlled by the life-time of DNA/membrane complex formation, J. Gene Med. 12 (2010) 117–125, https://doi.org/10.1002/jgm.1414.
[77] S. Satkauskas, Mechanisms of in Vivo DNA Electrotransfer: Respective Contributions of Cell Electropermeabilization and DNA Electrophoresis, Mol. Ther. 5 (2002) 133–140, https://doi.org/10.1006/mthe.2002.0526.
[78] D.A. Zaharoff, J.W. Henshaw, B. Mossop, F. Yuan, Mechanistic analysis of electroporation-induced cellular uptake of macromolecules, Exp Biol Med. 233 (2009) 94–105, https://doi.org/10.3181/0704-RM-113.Mechanistic.
[79] M. Cemazar, M. Golzio, G. Sersa, J.M. Escoffre, A. Coer, S. Vidic, J. Teissie, Hyaluronidase and collagenase increase the transfection efficiency of gene electrotransfer in various murine tumors, Hum Gene Ther. 23 (2012) 128–137, https://doi.org/10.1089/hum.2011.073.
[80] M. Golzio, M.P. Mora, C. Raynaud, C. Delteil, J. Teissié, M.P. Rols, Control by osmotic pressure of voltage-induced permeabilization and gene transfer in mammalian cells, Biophys. J. 74 (1998) 3015–3022, https://doi.org/10.1016/S0006-3495(98)78009-9.
[81] F.M. André, J. Gehl, G. Sersa, V. Préat, P. Hojman, J. Eriksen, M. Golzio, M. Cemazar, N. Pavselj, M.-P. Rols, D. Miklavcic, E. Neumann, J. Teissié, L.M. Mir, Efficiency of High- and Low-Voltage Pulse Combinations for Gene Electrotransfer in Muscle, Liver, Tumor, and Skin, Hum. Gene Ther. 19 (2008) 1261–1272, https://doi.org/10.1089/hum.2008.060.
[82] S. Haberl, D. Miklavčič, G. Serša, W. Frey, B. Rubinsky, Cell membrane electroporation-Part 2: The applications, IEEE Electr. Insul. Mag. 29 (2013) 29–37, https://doi.org/10.1109/MEI.2013.6410537.
[83] M. Kandušer, D. Miklavčič, M. Pavlin, Mechanisms involved in gene electrotransfer using high- and low-voltage pulses - An in vitro study, Bioelectrochemistry. 74 (2009) 265–271, https://doi.org/10.1016/j.bioelechem.2008.09.002.
[84] A. Donate, A. Bulysheva, C. Edelblute, D. Jung, M.A. Malik, S. Guo, N. Burcus, K. Schoenbach, R. Heller, Thermal Assisted In Vivo Gene Electrotransfer, Curr. Gene Ther. 16 (2016) 83–89, https://doi.org/10.2174/1566523216666160331125810.
[85] C. Mennuni, F. Calvaruso, I. Zampaglione, G. Rizzuto, D. Rinaudo, E. Dammassa, G. Ciliberto, E. Fattori, N. La Monica, Hyaluronidase increases electrogene transfer efficiency in skeletal muscle, Hum. Gene Ther. 13 (2002) 355–365, https://doi.org/10.1089/10430340252792495.